

Estimation of melt oxidation kinetics

J. Stuckert

Abstract

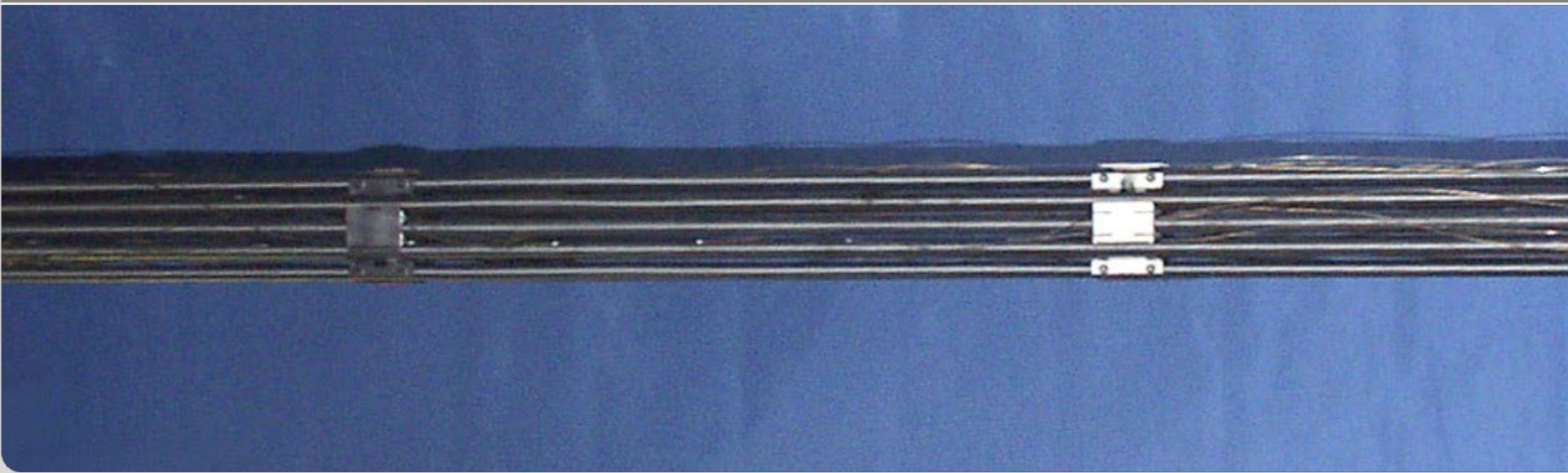
The analysis of the viscous melt behavior in the CORA and QUENCH bundles and the image analysis of the frozen melt show the formation of ceramic precipitates in the melt even in the molten state. The driving mechanism for the formation of precipitates in the melt is the temperature gradient at the oxide-melt interface. The high temperature Prater-Courtright correlation, used usually in computer codes to simulate the oxidation of Zr melt, was obtained based on the oxidation of very thin samples, which does not allow taking into account processes in the bulk melt. Simulation of the melt oxidation by the mechanistic SVECHA code, verified on the basis of many crucible tests, gives more correct result. This takes into account not only the formation of an external oxide layer around the molten pool, but also the formation of ceramic precipitation inside the melt. A numerical calculation carried out for the case with an operating temperature of 2473 K and a temperature gradient at the melt boundary of 50 K showed that the oxidation process occurs parabolically and three times faster than predicted by the Prater-Courtright correlation. The estimated activation energy for the melt oxidation correlation of Arrhenius-type proposed on the basis of SVECHA calculations is 85.9 kJ/mol, which is noticeably lower than the Prater-Courtright activation energy of about 110 kJ/mol.

Estimation of melt oxidation kinetics

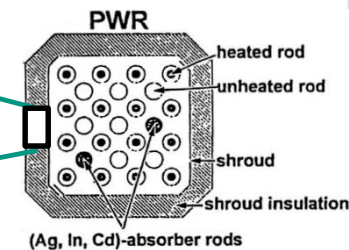
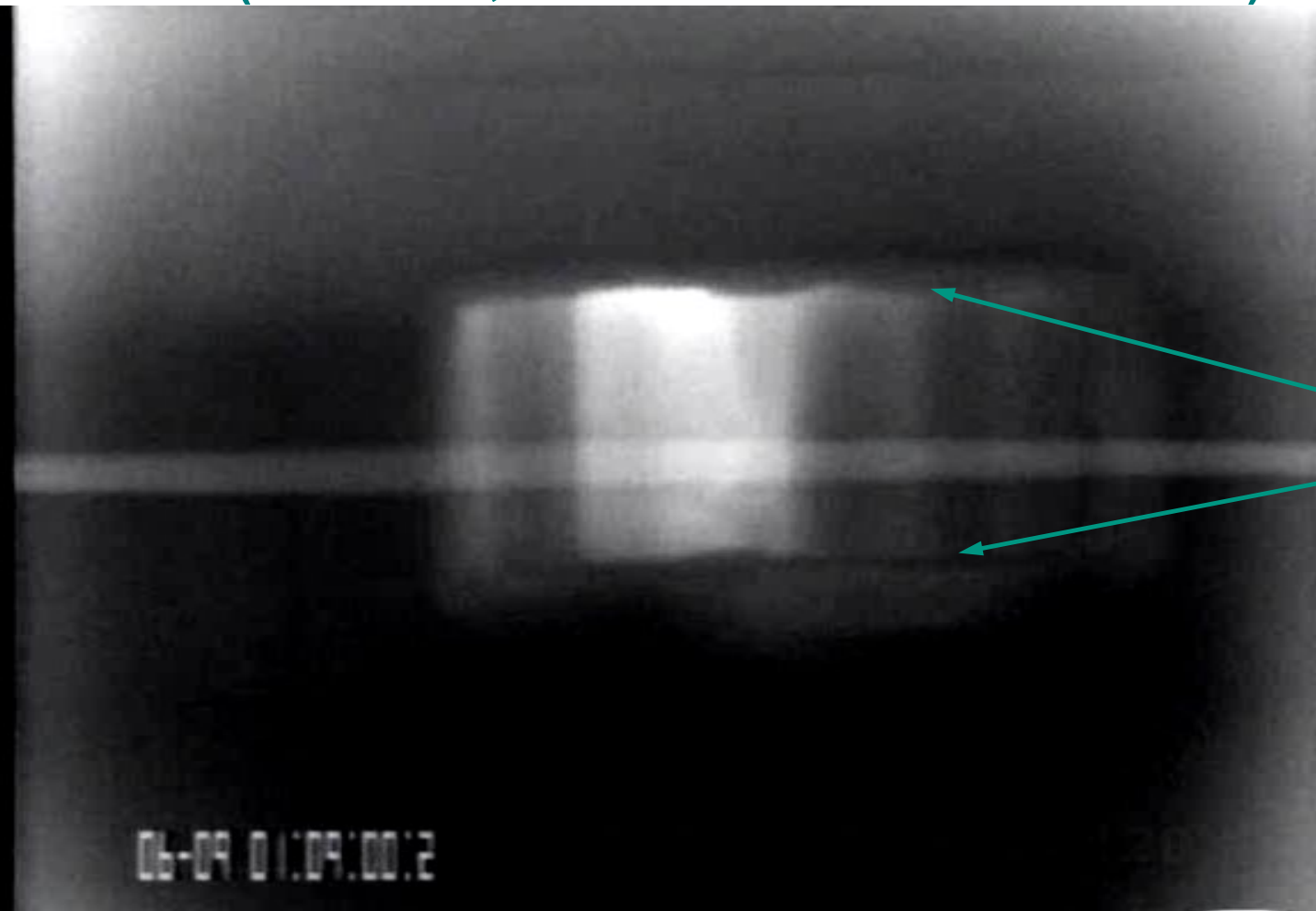
J. Stuckert

QWS-28, Karlsruhe

Institute for Applied Materials; Program NUSAFF

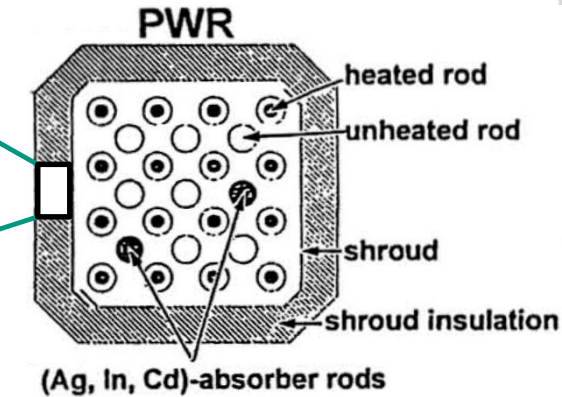
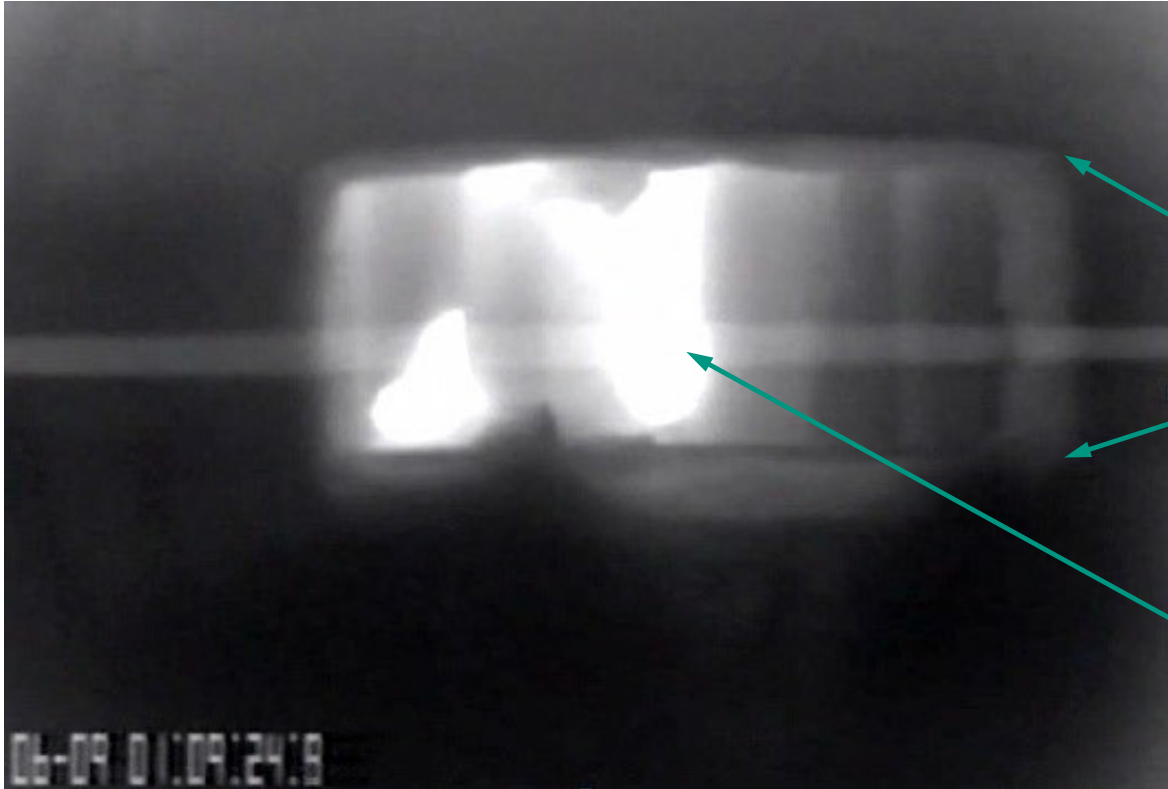


Melt relocation : rivulets and droplets in CORA-PWR tests (CORA-12, window at elevation 400 mm)



- rapid relocation of early metallic rivulets and later slowed relocation of partially oxidised rivulets
- relocation velocity of metallic rivulets $v_{\text{metal}} \approx 20 \text{ cm/s}$;
- melt with ceramic precipitates (with volumetric part f) $v \sim 1/\eta(f)$, η - viscosity of the melt

Melt relocation : rivulets and droplets in CORA-PWR tests (CORA-12, window at elevation 400 mm)



melt (Fe, Zr, U, (O), Ag, In, Cd,)

melt viscosity depends on temperature T and volume fraction of ceramic precipitates f

[M. Ramacciotti et al., NED 2001, [https://doi.org/10.1016/S0029-5493\(00\)00328-9](https://doi.org/10.1016/S0029-5493(00)00328-9)]: $\eta = \eta_{liq}(T) \cdot \exp(2.5 \cdot C \cdot f)$
with [Kaptay, 2004, <https://www.hanser-elibrary.com/doi/pdf/10.3139/146.018080>] $\eta_{liq}(T) = A(T) \cdot \exp(E/RT)$,

$A(T) \sim T_m^{-1/2}$, $E = 54(\text{Zr}) \dots 87(\text{ZrO}_2) \text{ kJ/mol}$ [Veshchunov et al., NED, 2008, <https://doi.org/10.1016/j.nucengdes.2007.10.015>], $C = 3 \dots 4.5$

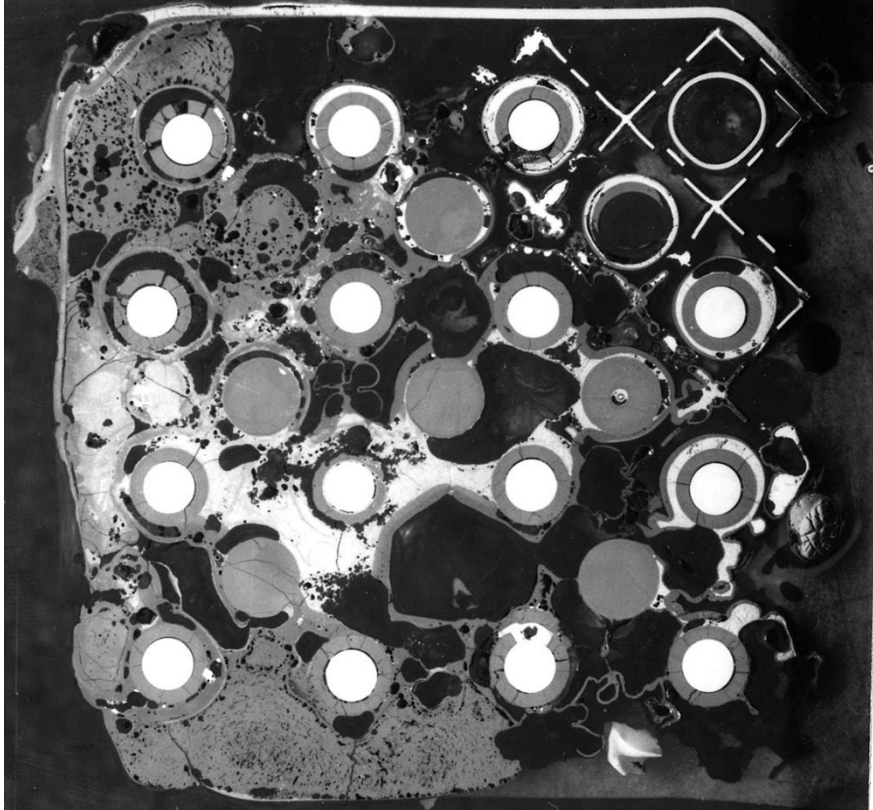
for Zr(O) at 2200 °C:

$$\eta_{Zr}(f=0) \approx 6 \text{ mPa}\cdot\text{s},$$

$$\eta_{Zr + ZrO_2}(f=0.2) \approx 30 \text{ mPa}\cdot\text{s} \rightarrow v_{melt} = v_{metal}/5 = 4 \text{ cm/s}$$

significant slower relocation than for the pure metal melt

Melt release outside of claddings and formation of molten pools frozen in steam atmosphere at middle bundle elevations

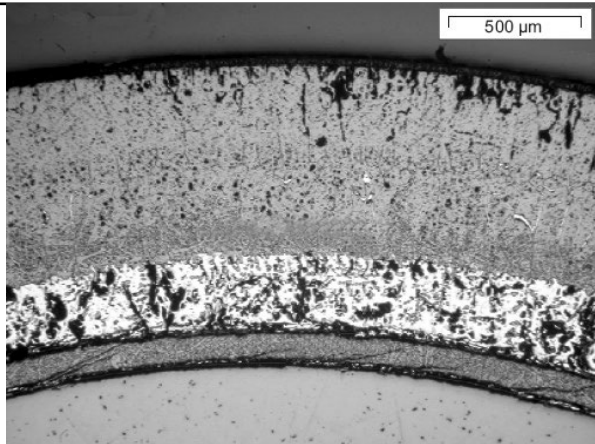


PWR CORA-15 ($T_{pct} \approx 2370\text{ K}$), elevation 480 mm: melt collection **at spacer grid**

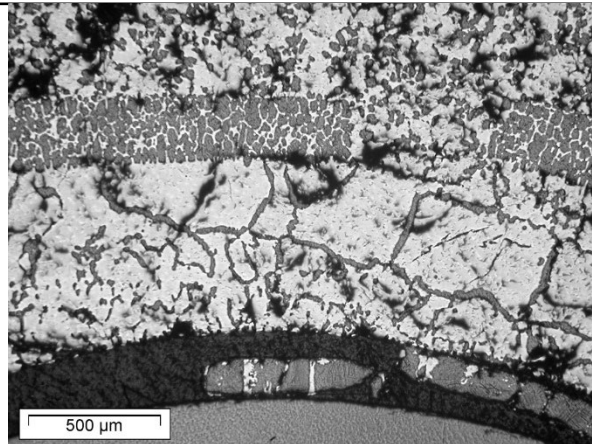


PWR QUENCH-11 ($T_{pct} \approx 2100\text{ K}$), elevation 837 mm: formation of large molten pools below the bundle hot region

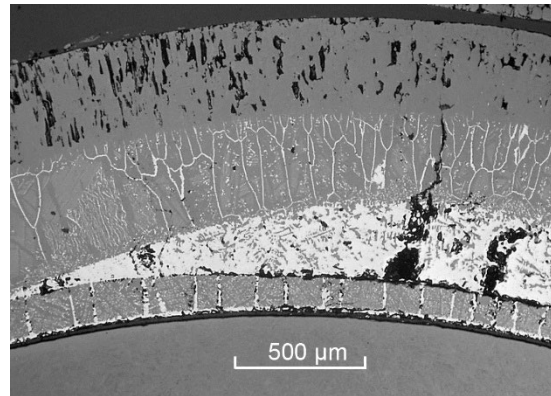
Cladding melt formation, oxidation and localization at the upper hottest bundle elevations for QUENCH bundles: formation of ceramic precipitates in the melt



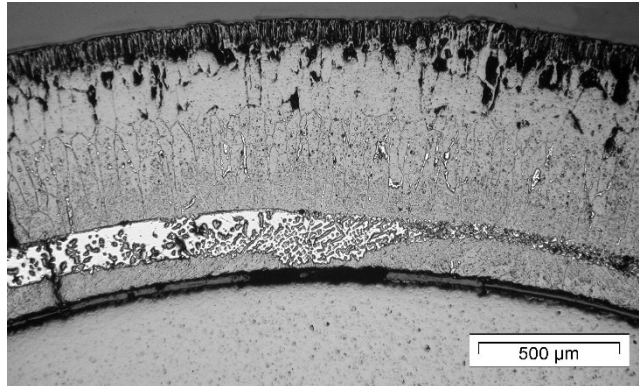
PWR QUENCH-06 (Zry-4), rod #12, 950 mm:
melt **captured** between clad oxide and pellet



VVER QUENCH-12 (E110), rod #8, 950 mm:
melt **partial release** through failed clad oxide

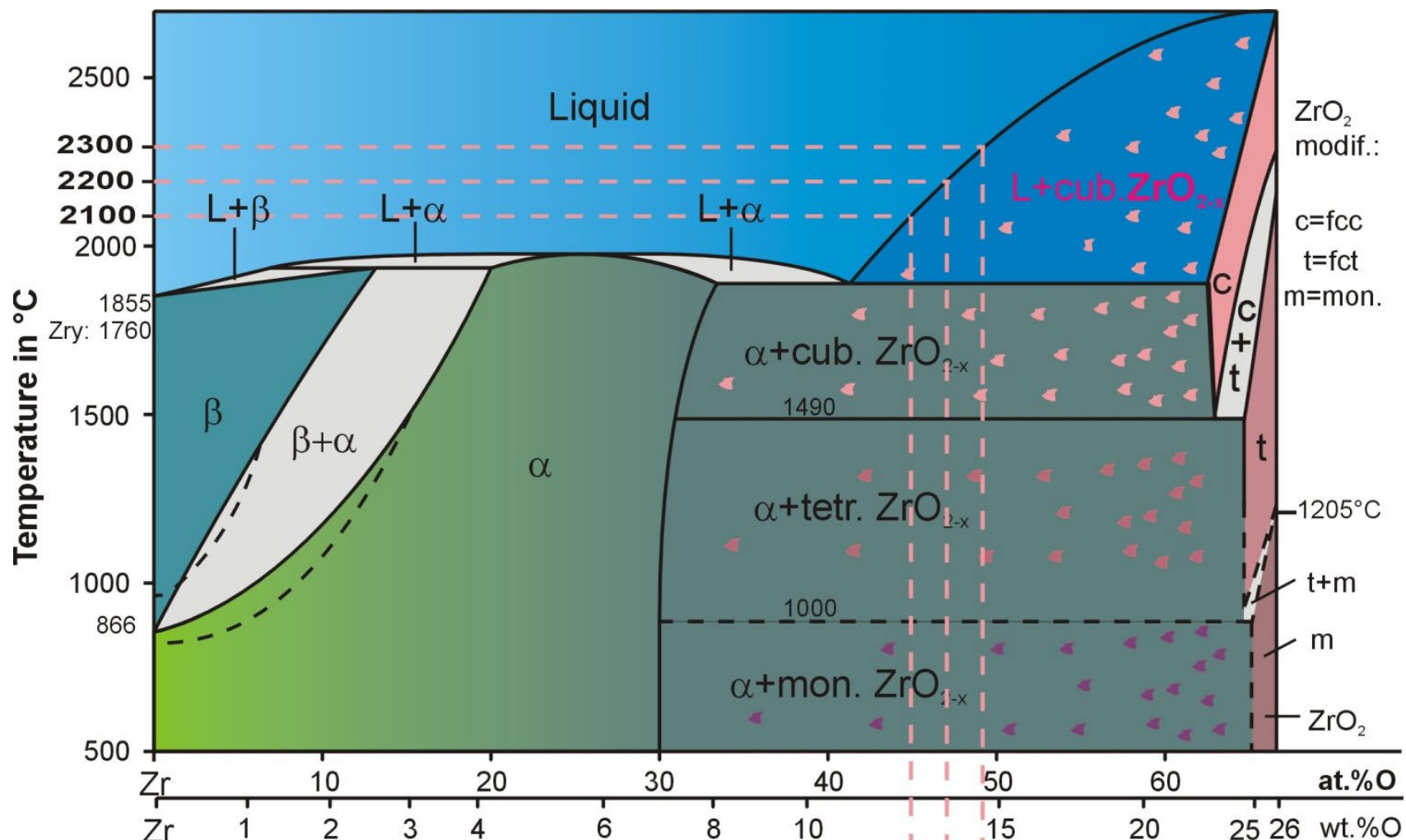


PWR QUENCH-14 (M5), rod #2, 1000 mm:
melt **captured** between clad oxide and pellet



PWR QUENCH-15 (ZIRLO), rod #17, 1000 mm:
melt **captured** between clad oxide and pellet

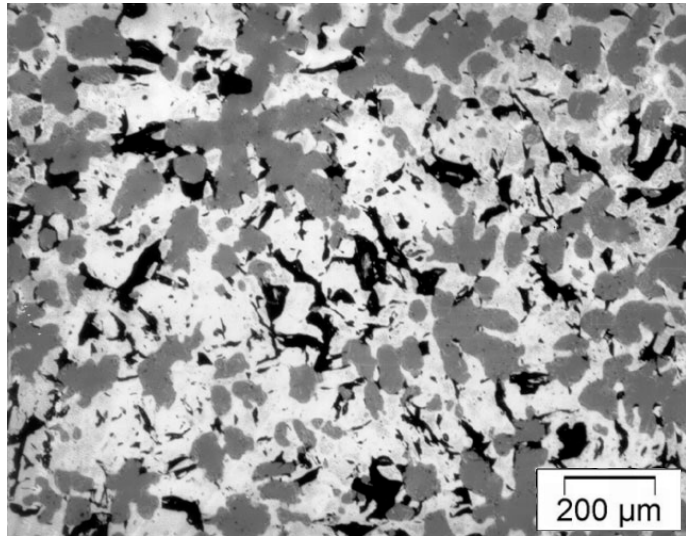
Simplified equilibrium Zr-O phase diagram



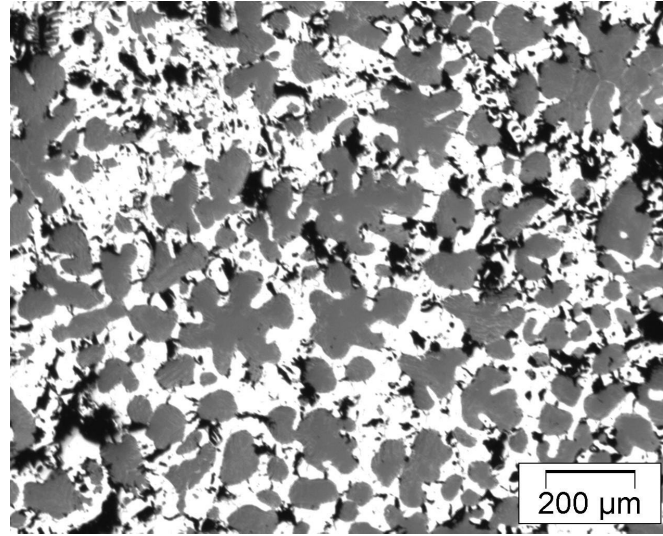
Solubility of oxygen in Zr liquid at 2100, 2200, 2300 °C:

| | | | |
|------|------|------|-------|
| 45.3 | 47 | 49.5 | at.%O |
| 12.7 | 13.5 | 14.7 | wt.%O |

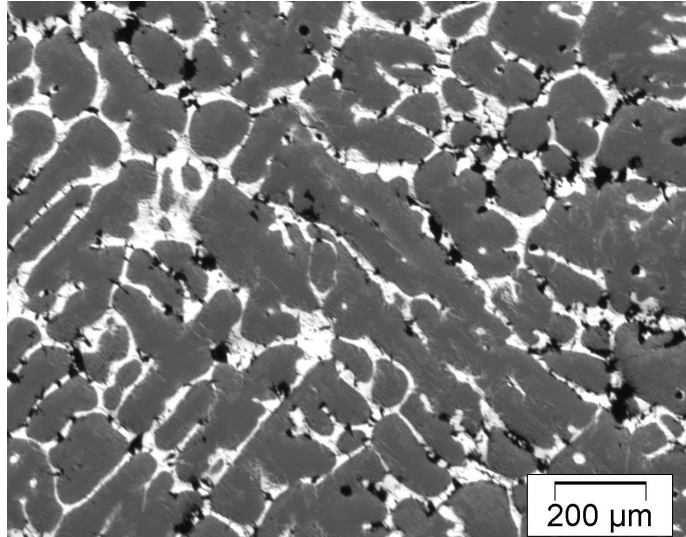
Crucible test, result of image analysis of the oxidized melt: partial formation of precipitates before cool-down (oversaturation)



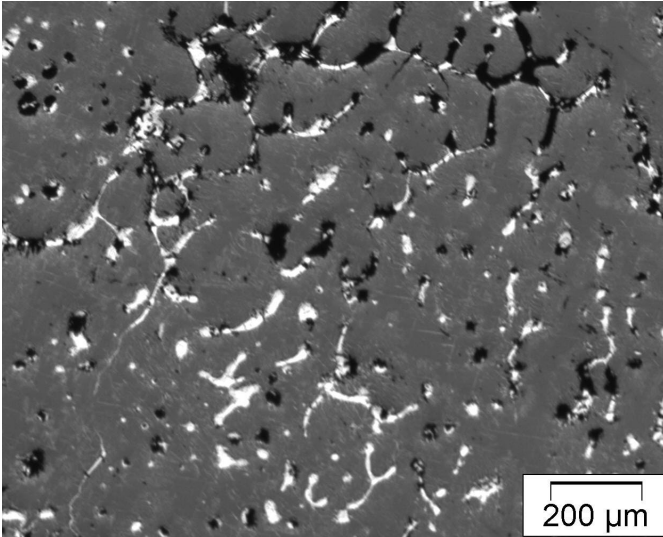
2100 °C, oxygen content **49 at%** (>solubility limit of 45%)



2100 °C, oxygen content **55 at%** (>solubility limit of 45%)



2200 °C, oxygen content **61.5 at%** (>solubility limit of 47%)



2200 °C, oxygen content **63.5 at%** (>solubility limit of 47%)

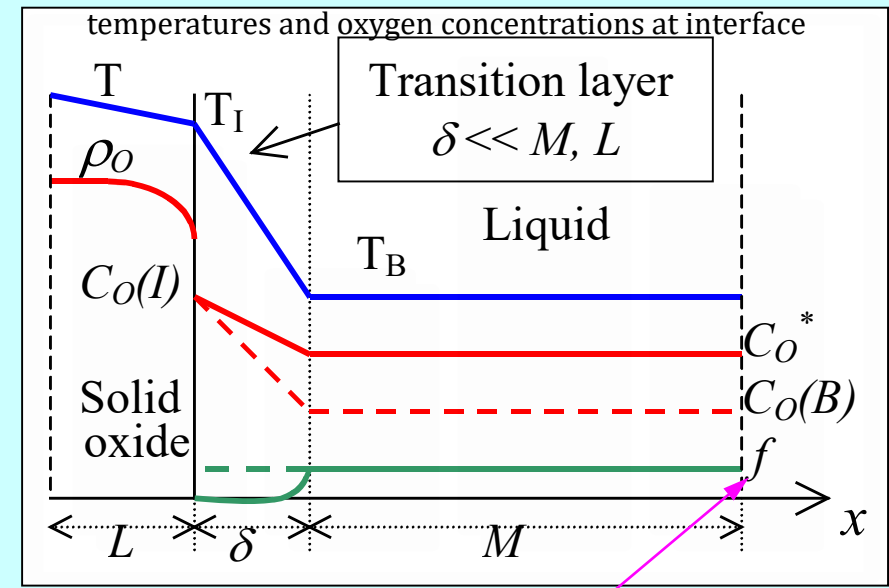
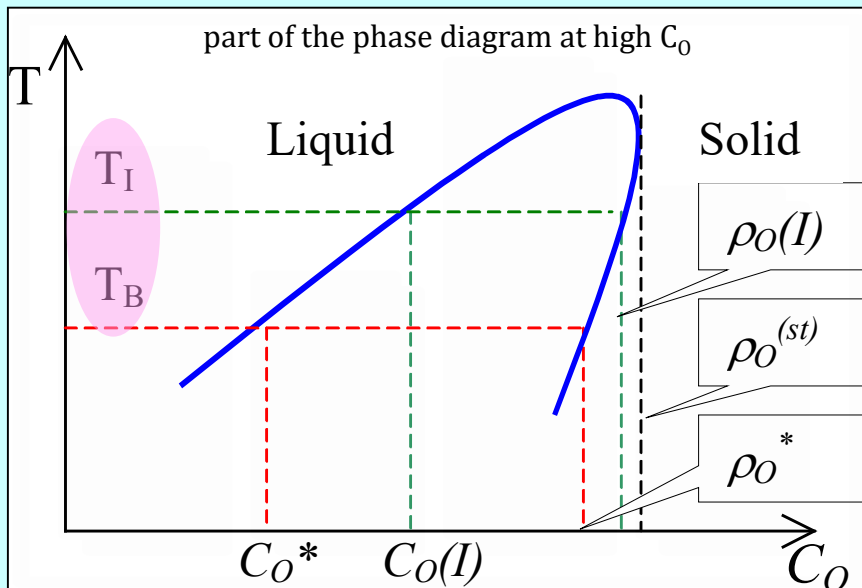


Mechanism of precipitates formation due to the temperature gradient at the liquid-solid interface: SVECHA model verified on the basis of crucible tests

[Veshchunov, Stuckert, Berdyshev, 2002, Karlsruhe, FZKA 6792,

<https://www.doi.org/10.5445/IR/270053667>

*possible reasons of the temperature gradient: exothermic reaction of steam with metal
and the axial temperature difference*



One-dimensional mass transfer equations in SVECHA during the precipitation stage

Mass balances

$$-D_0^{ZrO_2} \frac{\partial \rho_O}{\partial x} |_I - \rho_O(I) \frac{dL}{dt} = \frac{d}{dt} [c_O^* M (1-f) + \rho_O^* M f]$$

$$-\rho_{Zr} \frac{dL}{dt} = \frac{d}{dt} [c_{Zr}^* M (1-f) + \rho_{Zr} M f]$$

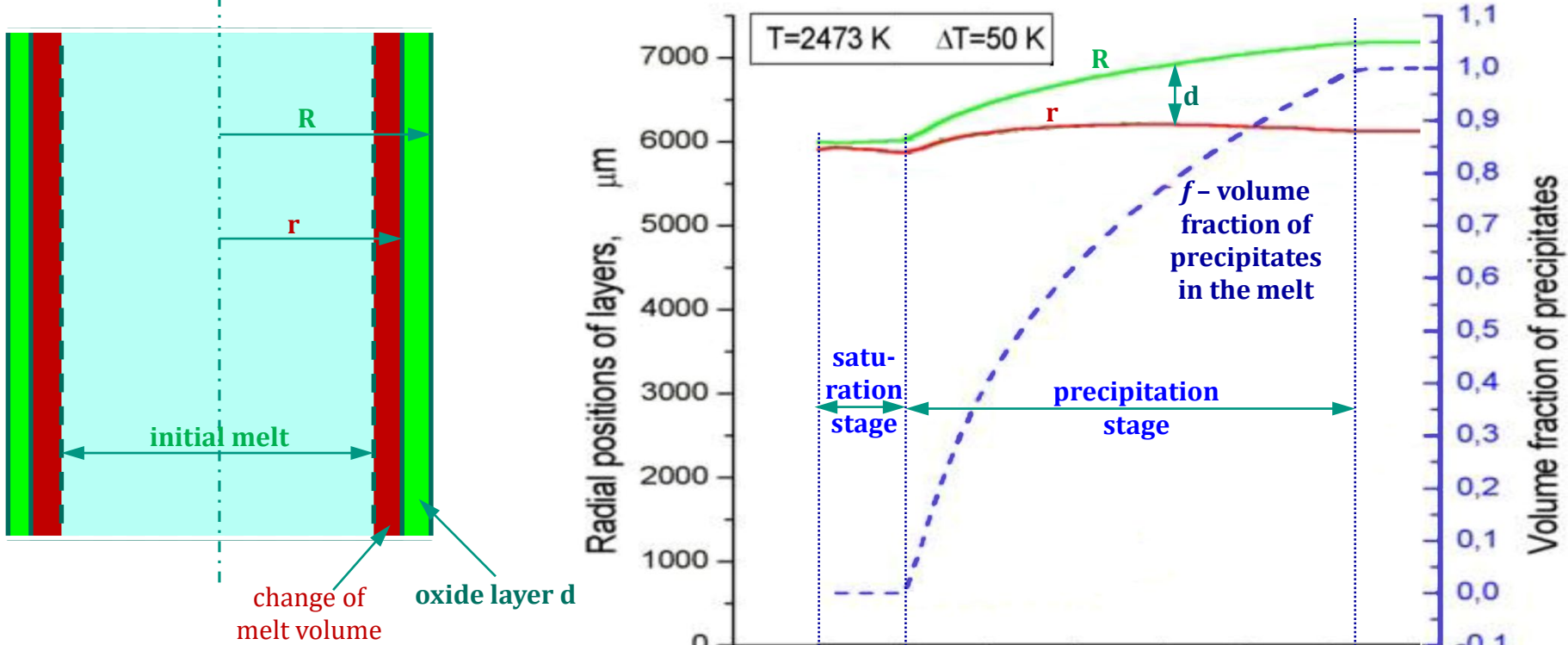
Flux matches

$$-D_0^{ZrO_2} \frac{\partial \rho_O}{\partial x} |_I - \rho_O(I) \frac{dL}{dt} = c_O(I) \left(u - \frac{dL}{dt} \right) + k_O e^{-2.5f} (c_O(I) - c_O^*)$$

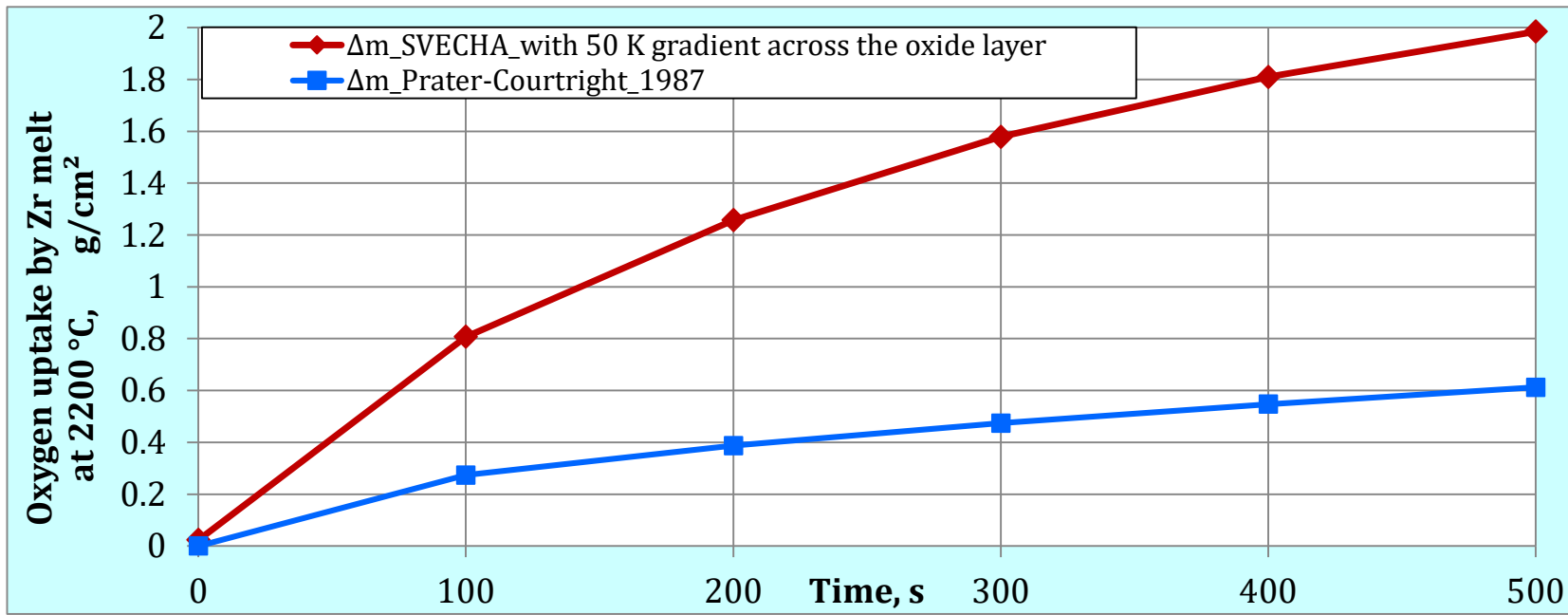
$$-\rho_{Zr} \frac{dL}{dt} = c_{Zr} \left(u - \frac{dL}{dt} \right),$$

u - net velocity of the melt, k - mass transfer coefficient in the melt

SVECHA modelling results of Zr melt oxidation at melt temperature 2473K and temperature drop in the transition boundary layer $\Delta T = 50$ K for cylindrical molten pool with $R_0=6$ mm



Oxygen uptake by molten pools at 2200 °C: comparison of two models (SVECHA vs. Prater-Courtright)



| t, s | mass gain by ZrO_2 layer Δm_{R-r} , g/cm^2 | mass gain by ZrO_2 precipitates in melt m_f , g/cm^2 | total mass gain Δm_{SVECHA} , g/cm^2 | Prater-Courtright mass gain Δm_{PC} , g/cm^2 | $\Delta m_{SVECHA}/\Delta m_{PC}$ |
|--------|--|--|--|--|-----------------------------------|
| 0 | 0.023 | 0 | 0.023 | 0 | |
| 100 | 0.057 | 0.751 | 0.807 | 0.274 | 3.0 |
| 200 | 0.088 | 1.169 | 1.257 | 0.387 | 3.2 |
| 300 | 0.120 | 1.458 | 1.578 | 0.474 | 3.3 |
| 400 | 0.153 | 1.657 | 1.809 | 0.547 | 3.3 |
| 500 | 0.182 | 1.803 | 1.984 | 0.612 | 3.2 |

➤ accelerated melt oxidation due to formation of ceramic precipitates: factor 3 in comparison to the Prater-Courtright

➤ suggested kinetics: $K_{mod}=5.74 \cdot \exp(-85900/RT)$, $g/cm^2/s^{0.5}$ (instead $K_{PC}=5.74 \cdot \exp(-109911/RT)$, $g/cm^2/s^{0.5}$)

Conclusions

- The analysis of the viscous melting behavior in bundles and the image analysis of the frozen melt show the formation of ceramic precipitates in the melt even in the molten state.
- The driving mechanism for the formation of precipitates is the temperature gradient at the oxide-melt interface.
- The high temperature Prater-Courtright correlation used usually in computer codes was obtained based on the oxidation of very thin samples, which does not allow taking into account processes in the bulk melt.
- Simulation of the melt oxidation by the mechanistic SVECHA code, verified on the basis of many crucible tests, gives more correct result. This takes into account not only the formation of an external oxide layer, but also the formation of ceramic precipitation inside the melt.
- A numerical calculation carried out for the case with an operating temperature of 2473 K and a temperature gradient at the melt boundary of 50 K showed that the oxidation process occurs parabolically and three times faster than predicted by the Prater-Courtright correlation.
- Activation energy of the new suggested correlation is 85.9 kJ/mol, which is noticeably lower than the Prater-Courtright activation energy of about 110 kJ/mol.
- It is advisable to carry out additional calculations to specify more precisely the activation energy and the pre-exponential factor in the correlation for different temperature gradients at the solid-melt interface.

Thank you for your attention

<http://www.iam.kit.edu/awp/163.php>

<http://quench.forschung.kit.edu/>